MODELLING OF THE LINEAR DC MACHINE USING NEWTONIAN AND LAGRANGE METHODS, AND APPLICATION OF A CONTROL FOR VELOCITY CONTROL TUNING

Teboho Lekeno (1130992)

***Abstract*— Linear DC Machine is a system used to introduce students to advanced modelling techniques to determine its model representation and design of a controller for it. Different methods of deriving the equations of motion for a system exist, in this paper, the Newtonian and the Euler-Lagrangian methods are applied. Unlike the Newtonian method, the equations of motion are obtained naturally in the Euler-Lagrange method. It is further shown in this report that the equations of motion obtained from the aforementioned methods are identical. The PID controller is introduced to tune velocity control of the system. Using the Trial and Error method to solve the coefficients of PID, it is observed that the solution found reduces the system into a PID controller. The results show PI controller to be better than PID in terms of velocity control tuning. It was possible to increase the P term further while meeting the requirements, which shows that P control can actually be an efficient solution for this application.**

I. INTRODUCTION

Processes such as motor velocity control and shaft positioning are usually slow. To improve the response of such plants requires a controller to adjust the performance of such systems

This paper aims to develop the equations of motion for the linear DC motor by applying Newtonian and Lagrangian mechanics. The raw behaviour of the obtained system will be modelled and a controller will be designed for tuning the velocity control of the plant.

II. BACKGROUND

A. Constraints and Assumptions

The following measures were imposed to limit the scope of the design.

- The bar of linear DC motor is moving up a fixed incline.
- The bar is cannot roll, it only slides.
- The only friction acting on the system is the viscous friction.

B. Success Criteria

The model of the system developed using Lagrange and Newtonian method should be the same. The velocity and positioning of the system should be analyzed and a suitable controller should be developed to tune the velocity control of the system to perfection.

School of Electrical & Information Engineering, University of the Witwatersrand, Private Bag 3, 2050, Johannesburg, South Africa

C. Literature Review

Processes such as motor speed controlling and rotational shaft positioning are naturally slow, thus they require a controller to adjust their performance to perfection. [1], [2] and [3] argues that the PID controller is better than PI in such applications by showing that the D term speed up the closed loop response. They both also highlight that the PID controller brings noise to the system since the derivative part amplify the noise margins. Their statements are contradicted by [4] and [5] who argues that the PI controller is better than PID in velocity control but PID is more flexible in positioning control. Those arguments will be used to determine and develop a controller suitable for tuning the velocity control of a plant.

Reference [6], [7] and [8] uses the Trial and Error method to determine the PID controller coefficients that efficiently satisfy the design requirements. The method first put the system into a rough solution and minor changes are applied to the controller coefficients to optimize the step response of the system. This method will be applied to obtain the controller.

III. SYSTEM MODEL USING EULER-LAGRANGE MECHANICS

Lagrange is an energy-based method, this implies it does not require vectors to determine system representation. This method is usually used to solve complicated systems [9]. The method will be applied to obtain the equations of motion for the linear DC machine.

A. Mechanical side

Figure 1, Appendix A shows the mechanical side of the system and its short brief. Considering Figure 1, the system can be fully presented by the generalized equation below

$$q(t) = [r(t)] \tag{1}$$

where r(t) is the position of the linear DC machine bar on the inclined rail of angle θ. The Lagrange equation for a system is then defined by the equation 2 where L is the Lagrangian define by equation 3 below

$$\frac{d}{dt}(\frac{\partial L}{\partial \dot{r_i}}) - (\frac{\partial L}{\partial r_i}) = Q_i \tag{2}$$

$$L = T - V \tag{3}$$

where T is the kinetic energy and V is the potential energy for the system. Considering Figure 1, it is observed that the kinetic and potential energies of the system can be expressed by equation 4 and 5 below.

$$T = \frac{1}{2}m\dot{r}^2 \tag{4}$$

$$V = mgrsin\theta \tag{5}$$

Substituting (4) and (5) into (3) gives the following Lagrangian

$$L = \frac{1}{2}m\dot{r}^2 - mgrsin\theta \tag{6}$$

Equation 7 and 8 provides the complete sub-equations computing the Lagrange equation.

$$\frac{d}{dt}(\frac{\partial L}{\partial \dot{r}}) = m\ddot{r} \tag{7}$$

$$(\frac{\partial L}{\partial r}) = mgsin\theta \tag{8}$$

Substituting (7) and (8) into (2) result in the Lagrange equation given by equation 9 below

$$m\ddot{r} - mgsin\theta = Q \tag{9}$$

Q is the external force applied to the system by the friction and the magnetic force applied by the electrical side of the system and it is obtained using equation 10 below

$$Q = Bli - b\dot{r} \tag{10}$$

where B is the magnetic flux density, l is the length of the bar, i is the current in the system and b is the coefficient of friction.

B. Electrical side

Figure 2, Appendix A shows the electrical side of the system, which forms the second equation of the Lagrange shown by represented by equation 11 below

$$\frac{d}{dt}(\frac{\partial L}{\partial \dot{q}}) - (\frac{\partial L}{\partial q}) + \frac{\partial P}{\partial \dot{q}} = Q \tag{11}$$

where P is the power dissipated into the resistor characterized by equation 12 below.

$$P = \frac{1}{2}R\dot{q}^2 \tag{12}$$

The term with power in the second Lagrange equation is the only one existing on the left-hand side since there is no kinetic or potential energy on the electrical side. The solution to this term is shown in equation 13 below.

$$\frac{\partial P}{\partial \dot{q}} = R\dot{q} \tag{13}$$

The remaining Q term from the right-hand side of the equation found by subtracting the back emf from the supply voltage as shown below

$$Q = V_{bat} - Bl\dot{r} \tag{14}$$

therefore substituting (13) and (14) into (11) and taking the current as the subject of the formula result into equation 15 below since i is equal to $\dot{q}$.

$$i = \frac{V_{bat} - Bl\dot{r}}{R} \tag{15}$$

Finally, substituting (15) into (10) and applying the resultant Q into (9) gives the complete solution shown by equation 16 which can further be factorized to equation 17 below.

$$m\ddot{r} - mgsin\theta = Bl(\frac{V_{bat} - Bl\dot{r}}{R}) - b\dot{r} \tag{16}$$

$$m\ddot{r} + (\frac{B^2l^2}{R} + b)\dot{r} = \frac{BlV_{bat}}{R} + mgsin\theta \tag{17}$$

IV. SYSTEM MODEL USING NEWTONIAN MECHANICS

In this section, the Newtonian approach is used to obtain the equations of motion for the system. Figure 3, Appendix A shows the free-body diagram of all forces acting on the linear DC machine bar. Newton second law is portrayed by equation 18 below.

$$F_{net} = m\ddot{r} \tag{18}$$

where F_{net} is the sum of all the applied forces ($F_{applied}$) deducting the forces that oppose the motion of the bar, F_f. The sum of all forces applying and preventing motion is shown by equation 19, 20, and 21 shows the net force.

$$F_{applied} = Bli - mgsin\theta \tag{19}$$

$$F_f = b\dot{r} \tag{20}$$

$$F_{net} = Bli - mgsin\theta - b\dot{r} \tag{21}$$

Substituting (21) into (19) gives the equation of motion for the system.

$$Bli - mgsin\theta - b\dot{r} = m\ddot{r} \tag{22}$$

Using Kirchhoff law to determine the current across the electrical side will lead to the same solution in equation (15), therefore substituting it into (22), results into the complete Newtonian equation shown by equation 23.

$$m\ddot{r} + (\frac{B^2l^2}{R} + b)\dot{r} = \frac{BlV_{bat}}{R} - mgsin\theta \tag{23}$$

The solution of Newtonian is exactly equal to that Lagrange as required.

V. UNCOMPENSATED LINEAR DC MOTOR MODELLING

A. Machine Parameters

Table 1, Appendix a showcases the parameters of the machine for which the modelling will be carried out.

B. Transfer Function

Equation 17 can be used to obtain the transfer function of the system but there is a constant gravitational force which cannot allow the realization of the transfer function. The total voltage of the system V_{bat} can be expressed by equation 24 below

$$V_{bat} = V_{motion} + V_{potential} \tag{24}$$

where $V_{potential}$ is the voltage required to create the magnetic potential that will hold the bar in equilibrium against gravitational force and V_{motion} is voltage required to create the force required to move the bar.

Substituting (24) into (17) we obtain equation 25.

$$m\ddot{r} + (\frac{B^2l^2}{R} + b)\dot{r} = \frac{Bl(V_{motion} + V_{potential})}{R} - mgsin\theta \tag{25}$$

Since the magnetic potential should balance the gravitational force, this means their sum should equal to zero, therefore the require $V_{potential}$ is expressed by equation 26 below.

$$V_{potential} = \frac{mgRsin\theta}{Bl} \tag{26}$$

Therefore equation 25 reduces to equation 27 below and the transfer function can thus be obtained from it.

$$m\ddot{r} + (\frac{B^2l^2}{R} + b)\dot{r} = \frac{BlV_{motion}}{R} \tag{27}$$

Taking the Laplace of the transform of (27), the transfer function of the system considering V_{motion} as the input and velocity $(\dot{r})$ as the output is expressed by equation 28 below

$$G_p = \frac{\frac{Bl}{B^2l^2+Rb}}{\frac{mR}{B^2l^2+Rb}s + 1} \tag{28}$$

where the time constant (τ) and the DC Gain (K) are expressed by equation 29 and 30 below.

$$\tau = \frac{mR}{B^2l^2 + Rb} \tag{29}$$

$$K = \frac{Bl}{B^2l^2 + Rb} \tag{30}$$

Figure 4, Appendix B showcases the step response of the system speed, with the rise time of 1.2 seconds, settling time of 2.14 seconds and the overshoot of 0%. Figure 5, Appendix B showcases the step response of the system bar displacement.

VI. DESIGN OF THE LINEAR DC MACHINE VELOCITY CONTROLLER SYSTEM

This section aims to design the controller for the velocity of the system. This controller should improve the rise time, settling time and introduce less overshoot or none at all.

A. Design Requirements

In order to improve the performance of the initial system, a controller will be necessary. The following requirements are imposed on the final system containing the controller.

1) The complete system is required to have a rise time less than 0.6 seconds.
2) It is allowed to have a steady state error less than 1%
3) It should reduce the settling time to be less than 1.5 seconds.

B. Design using PID Controller

The PID controller will be used to compensate for the system. The PID derivative part allows extra control action faster compared to the P and PI [10]. The standard equation for the PID controller in the Laplace domain is described by the equation below

$$U(s) = (K_p + \frac{K_I}{s} + s{\cdot}K_d){\cdot}E(s) \tag{31}$$

where the constants K_p, K_I, and K_d belongs to the proportional, integral, and derivative. The closed loop system of the plant characterized by equation 28 with a PID controller is therefore expressed by the simplified overall transfer function in equation 32 below.

$$G(s) = \frac{\frac{(K_p{\cdot}s+K_I+K_ds^2){\cdot}K}{\tau+K_d{\cdot}K}}{s^2 + (\frac{1+K_p{\cdot}K}{\tau+K_d{\cdot}K}){\cdot}s + \frac{K_I{\cdot}K}{\tau+K_d{\cdot}K}} \tag{32}$$

Figure 6, Appendix C shows the model of the system with the PID controller.

1) Determining Coefficients of the PID Controller: To determine the coefficients of the PID that best suit the design requirements, the Trial and Error method aforementioned will be applied. Before the process commences, the knowledge of the damping ratio (ζ) and natural frequency (ω_n) of the system is required. These parameters are calculated using (33) and (34) below

$$\zeta = \sqrt{\frac{(ln\frac{PO}{100})^2}{(ln\frac{PO}{100})^2 + \pi^2}} = 0.6901 \tag{33}$$

$$\omega_n = \frac{1 - 0.4167\zeta + 2.917\zeta^2}{t_{rise}} = 3.5027 \tag{34}$$

where t_{rise} is the rise time and PO is the percentage overshoot.

With the knowledge of ω_n and ζ the Trial and Error can therefore be applied. The process start with selecting and varying the value of K_I while K_p and K_d depend upon it with the following equations,

$$K_d = \frac{K_I}{\omega_n^2} - \frac{\tau}{K} \tag{35}$$

$$K_p = \frac{2\zeta\omega_n(\tau + K_d{\cdot}K)}{K} - \frac{1}{K} \tag{36}$$

The values of K_I were varied from 0 to 8 using MATLAB/SIMULINK. The behaviour of the system with K_I values between 0-3 was unsatisfactory and unacceptable. The system started to behave better when the value of K_I reaches 4 and increase further. When the value of K_I increases the rise and settling time of the system decreases which is a beneficial feature for the system but at the cost of increasing percentage overshoot, this results can be observed in Figure 7, Appendix C. Table 2, Appendix D records the data of rise time, settling time and percentage overshoot of the step response for K_I values aforementioned. It is observed from the table that system requirements are mostly satisfied when K_I is equal to 5, the Trial and Error method will then be applied to improve the performance of this partial solution.

The final optimum value of K_i was found to be 5.72, with a rise time of 0.388 seconds, 9.55% overshoot and settling time of 1.59 second. Figure 8, Appendix C showcases the response with an optimum value of K_I found. Equations (35) and (36) are no longer applicable after the value K_i is locked. K_p and K_d are now slightly varied with help of Table 3, Appendix D. The corresponding values of K_d and K_p at the partial solution were found to be 0 and 1.4 respectively which shows this solution reduces the system to the PI controller. Appendix C shows the impact of this PID constants on the design requirements.

The partial solution of the system is legitimized by Figure 9 and 10 in Appendix D. Figure 9 results were obtained by setting the value of K_p to zero, with a locked value of K_I and varying K_d. It is observed that increasing the value of K_d increases the rise time, settling time and shift the system offset from the origin. Even though the overshoot reduces with increasing K_d, it introduces noise to the system. These results show that partial solution results are legit to select K_d value as zero as hampers the system instead of perfecting it. Figure 10 results were obtained by setting the value of K_d to zero and varying the K_p. The results shows that increasing the value of K_p reduces the overshoot and rise time, the settling time is also reduced but also increase when K_p reach a certain bound. This results also show that the partial solution is legit by involving K_p since its behaviour is essential to allow the system to reach requirements. There is no curve from Figure 9 and 10 that surpassed the quality of the current partial solution.

From the aforementioned results, it is clear now that only the value of K_p needs to changed to perfect the system. Figure 11, Appendix E showcases the step response of the system for different values of K_p closer to perfecting the system. It is observed that the system meets the design requirements when the value of K_p is equal to 1.92. Figure 12, Appendix E shows the selected step response, which will give the final system details. With reference to that step response, the system will achieve a rise time of 0.373 seconds, overshoot of 4.96% and settling time of 1.58% within the 1% steady state error. The results fully satisfy and tally with the requirements.

With all the values of constants in equation 32 now known, the final system equation is then represented by equation 37 below.

$$G(s) = \frac{4.1143s + 12.2571}{s^2 + 5.9430s + 12.2571} \tag{37}$$

VII. ANALYSIS OF RESULTS

The equations of motion for the linear DC motor using the Lagrange and Newtonian method resulted in the same solution. The Lagrange method was found to be more efficient than Newtonian since it did not require the use of vectors compared to Newtonian, the equation of motions using it were naturally obtained. This observation tally with conclusion of [9].

Using Trial and Error method to determine the coefficients of PID that brings the system into partial solution using MATLAB/SIMULINK by varying the value of K_I, it was observed that the partial solution lies on step response of K_I equal to 5 (as seen in Figure 6, Appendix C) while K_p and K_d where depending on that value. The MATLAB calculation for that corresponding curve showed the value of K_d to be zero which highlights that the solution of the control should be a PI instead of PID, this solution proves the argument of [4] and [5] aforementioned to be valid. Minor changes were performed to perfect the partial solution, and the system managed to satisfy all the design requirements as seen in Figure 12, Appendix E.

To ensure that PID is not a conducive solution, the value of K_d was slowly increased while observing the changes it introduces into the system response with K_I and K_p kept constant. It was observed that D term introduces noise into the system. Even though the noise decreases with increasing K_d the settling time was quickly increasing beyond requirements. This results contradicted the argument of [1], [2] and [3] of PID being better than PI, but their statement about PID bringing noise to the system was observed in the results as seen in Figure 9, Appendix D.

A remarkable discovery was observed while tuning the value of K_p to perfect the system. Even though the solution that fully satisfies the imposed requirements was obtained; increasing the value K_p from that solution did not bring negative effects on the results, instead it further reduces the

rise time, settling time and the overshoot. When the value of K_p approaches infinity the overshoot disappeared, the rise time and settling time were also approaching zero, these results are shown in Figure 13, Appendix F. This means the controller turns into a P controller. This observation was further enhanced by taking the limit of K_p as it approaches infinity on the system closed-loop transfer function in (32), the mathematical proof in Appendix F also showed the transfer function being reduced into the closed loop transfer function with P controller. These findings show that a P controller can best satisfy the requirements as well, but in reality it impossible to have the infinite gain.

VIII. FUTURE RECOMMENDATIONS

In complex systems it becomes difficult to obtain the complete equations that define the system using Newtonian modelling since it requires the use of vectors are the modeller should have the knowledge of all the forces acting upon that system. Therefore it is recommended to use the Lagrange modelling since equations of naturally obtain and has the ability to prevail all components a modeller can somehow not realize using Newtonian method.

Trial and Error performance and results are optimal when the probability of obtaining the valid solution are high, however it is not a good practice to use it in problems that does not give multiple opportunities to obtain the solution. There exist other methods that could be used to determine controller coefficients and compare with the Trial Error such as Ziegler-Nichols and Cohen-Coon. Due to time constraints their application on this paper was impossible.

IX. CONCLUSIONS

In this paper, Lagrange and Newtonian methods were introduced to obtain the equation of motion that describe the linear DC motor on a fixed incline. Lagrange method was found more flexible as the equations of motion are obtained naturally from it. The PID controller was introduced introduces to tune the velocity control of the system. Trial and Error method was applied on MATLAB/SIMULINK software to determine the optimal coefficients of the PID that will satisfy the design requirements. The results obtained showed the control to optimal when the D term is zero which leads the solution to a PI controller. This solution is considered valid as PI is naturally better than PID when it comes to speed tuning. It recommended to use alternative approach to replace Trial and Error method in applications where there are limited ways to a solution.

REFERENCES

[1] A. O'Dwyer. *Handbook of PI and PID controller tuning rules*. Imperial College Press, 2009.

[2] S. Duman, D. Maden, and U. Güvenç. "Determination of the PID controller parameters for speed and position control of DC motor using gravitational search algorithm." In *2011 7th International Conference on Electrical and Electronics Engineering (ELECO)*, pp. I–225. IEEE, 2011.

[3] K. S. Rao and R. Mishra. "Comparative study of P, PI and PID controller for speed control of VSI-fed induction motor." *International Journal of Engineering Development and Research*, vol. 2, no. 2, pp. 2740–2744, 2014.

[4] H. Controls. "Why industry choose PI rather than PID or PD?", March 2013. URL `https://www.plctalk.net`.

[5] maplesoft. "PID Control.", March 2019. URL `https://www.maplesoft.com`.

[6] N. Kuyvenhoven. "PID tuning methods an automatic PID tuning study with MathCad." *Calvin college ENGR*, vol. 315, 2002.

[7] R. Bhat. "Time and Frequency Response Analysis of PID Controller." *Journal of Electronic Systems Volume*, vol. 2, no. 2, p. 75, 2012.

[8] S. Temel, S. Yağli, and S. Gören. "P, PD, PI, PID CONTROLLERS." *Middle East Technical University, Electrical and Electronics Engineering Department*, 2013.

[9] C. G. Bolívar-Vincenty and G. Beauchamp-Báez. "Modelling the ball-and-beam system from newtonian mechanics and from lagrange methods." In *12th Latin American and Caribbean Conference for Engineering and Technology (LACCEI2014), Guayaquil, Ecuador*. 2014.

[10] D. E. Rivera, M. Morari, and S. Skogestad. "Internal model control: PID controller design." *Industrial & engineering chemistry process design and development*, vol. 25, no. 1, pp. 252–265, 1986.

APPENDIX A

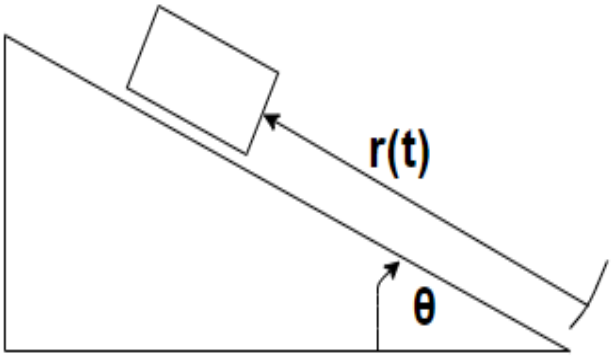

Figure 1: linear DC motor mechanical side diagram.

The bar slips on the rail with an incline under the influence of the frictional force. Due to the incline, the potential energy is present in the system and the magnetic force act as the applied force to control the movement of the bar.

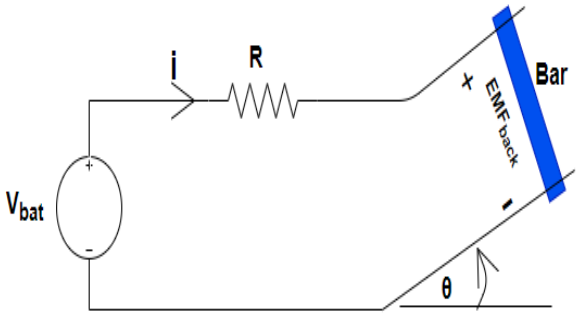

Figure 2: linear DC motor electrical side diagram.

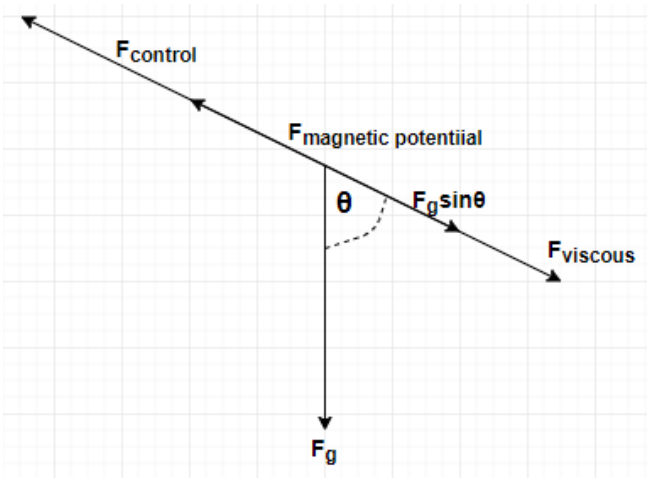

Figure 3: linear DC motor free body diagram.

APPENDIX B

Table 1: Parameters for the linear DC motor.

PARAMETERS	VALUE
Mass (m)	0.280kg
Length (l)	0.9m
Resistor (R)	1.2Ω
Voltage (V_{motion})	5V
Viscous coeffcient (b)	0.08

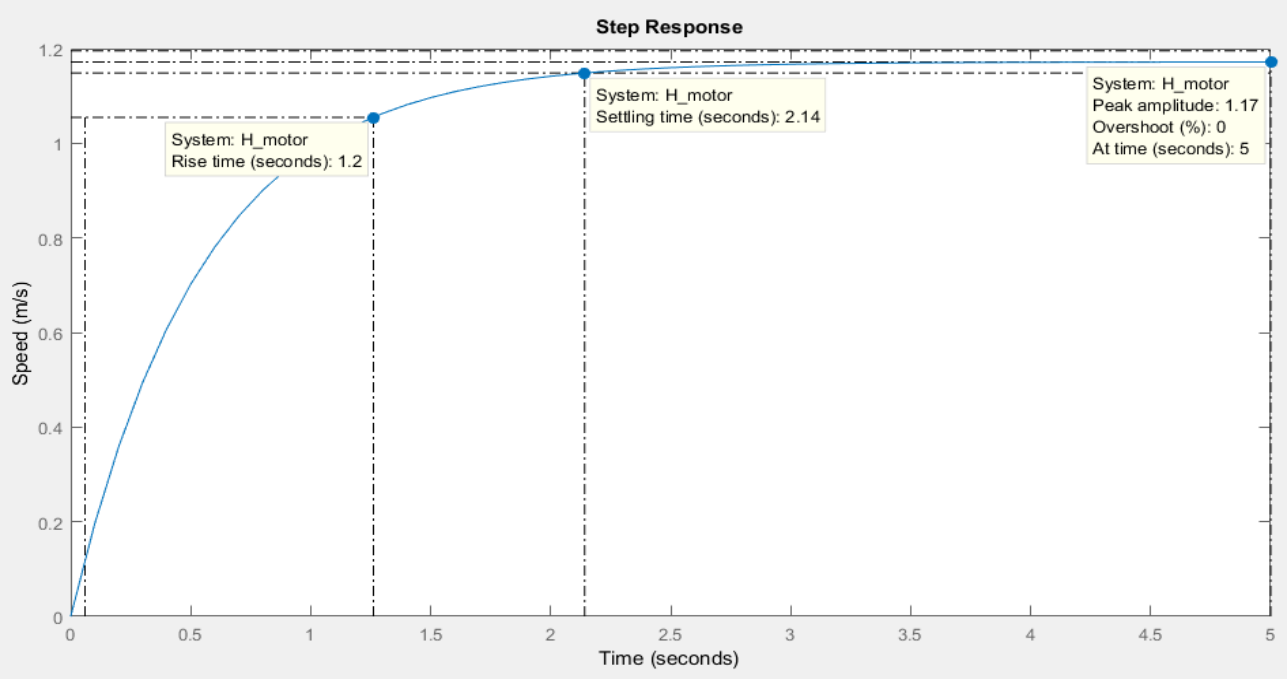

Figure 4: Uncompensated system velocity step response.

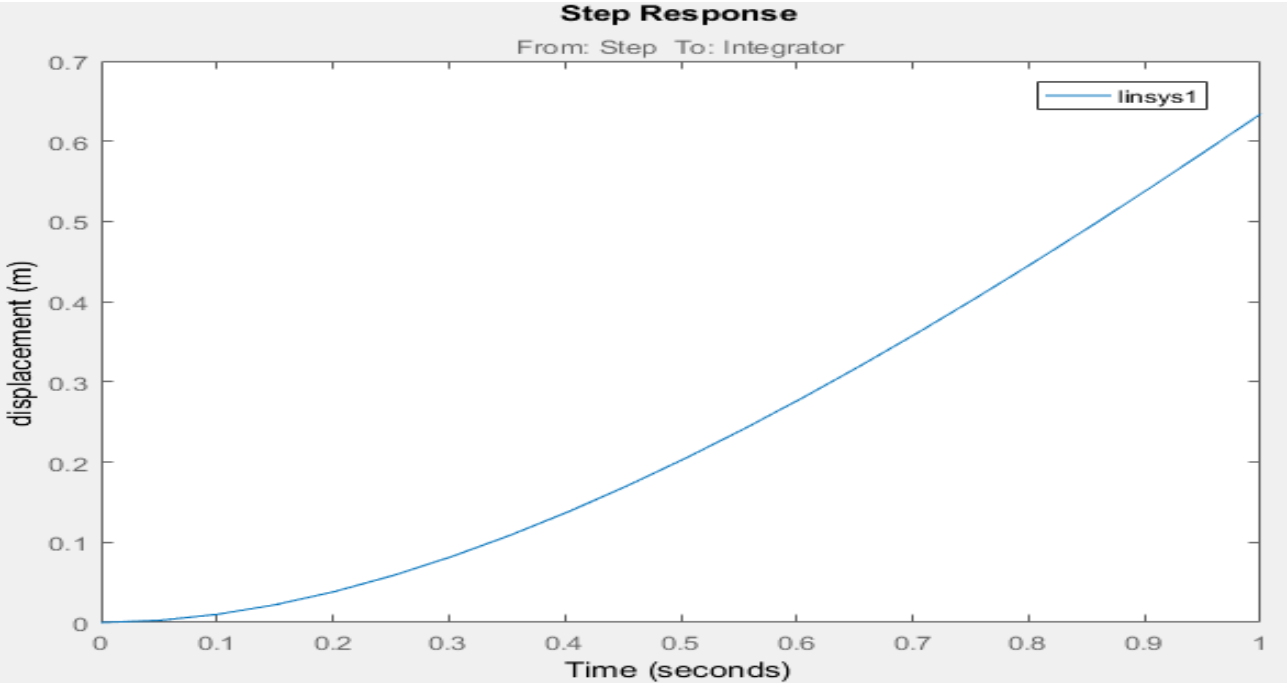

Figure 5: Uncompensated system displacement step response.

APPENDIX C

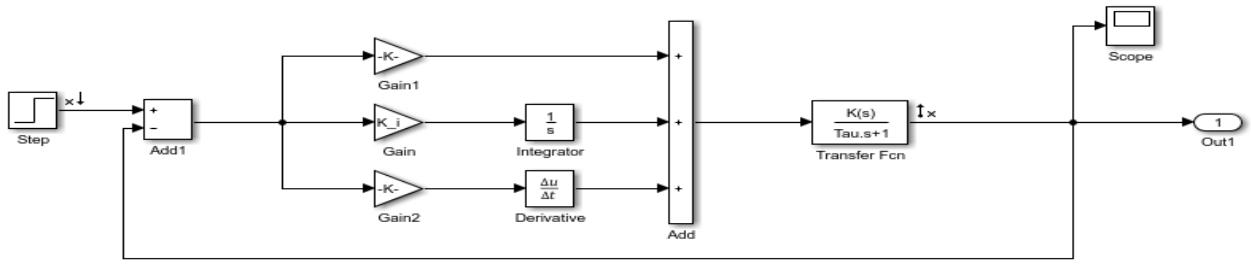

Figure 6: Plant with PID controller.

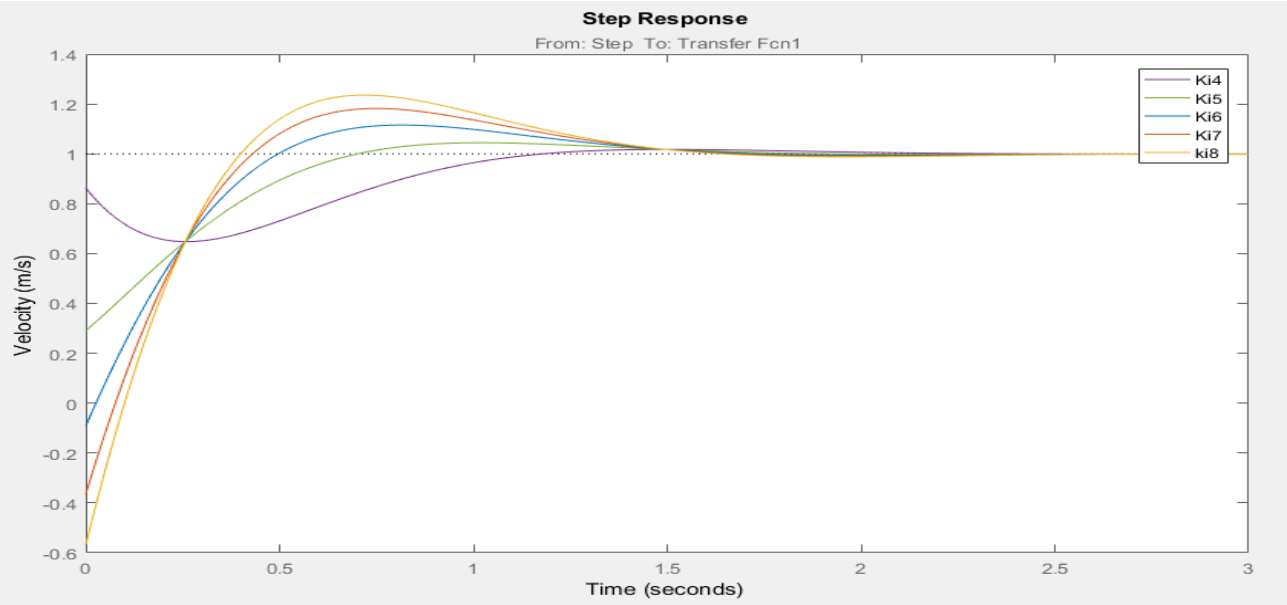

Figure 7: Step response for varies values of K_I.

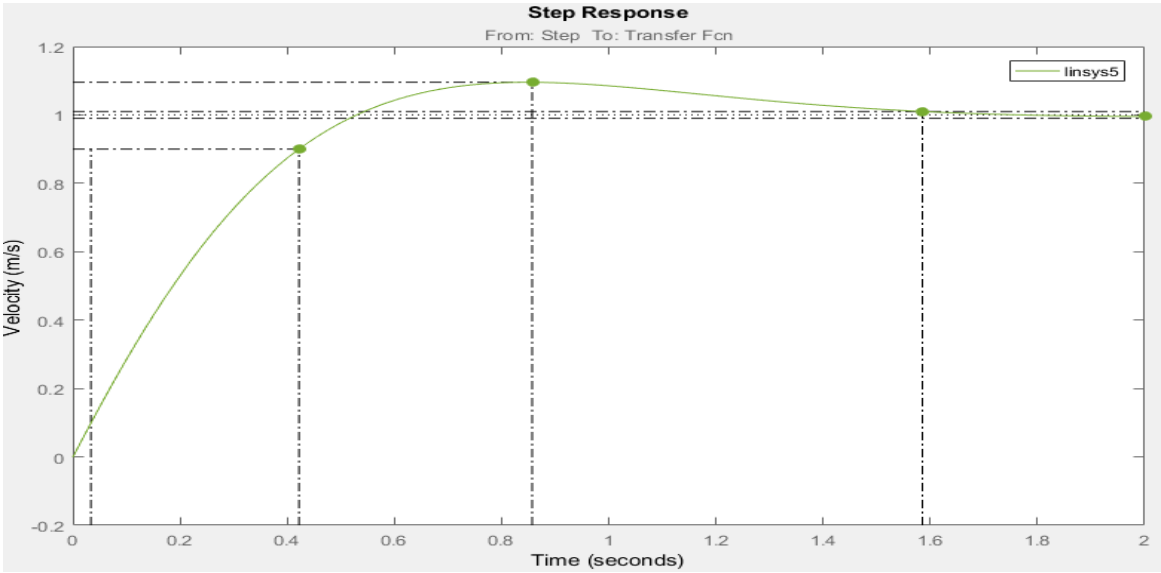

Figure 8: Step response for varies values of K_I.

APPENDIX D

Table 2: Step response data for various values of K_I.

K_I value	Rise time (s)	Overshoot (%)	Settling time (s)
4	1.10	1.74	1.97
5	0.56	4.5	1.55
6	0.37	11.6	1.46
7	0.35	18.2	1.43
8	0.33	23.6	1.42

Table 3: Effect of PID on the Design requirements.

	Rise time	Steady State	Overshoot
P	Decrease	Decrease	Increase
I	Decrease	Eliminated	Increase
D	None	None	Decrease

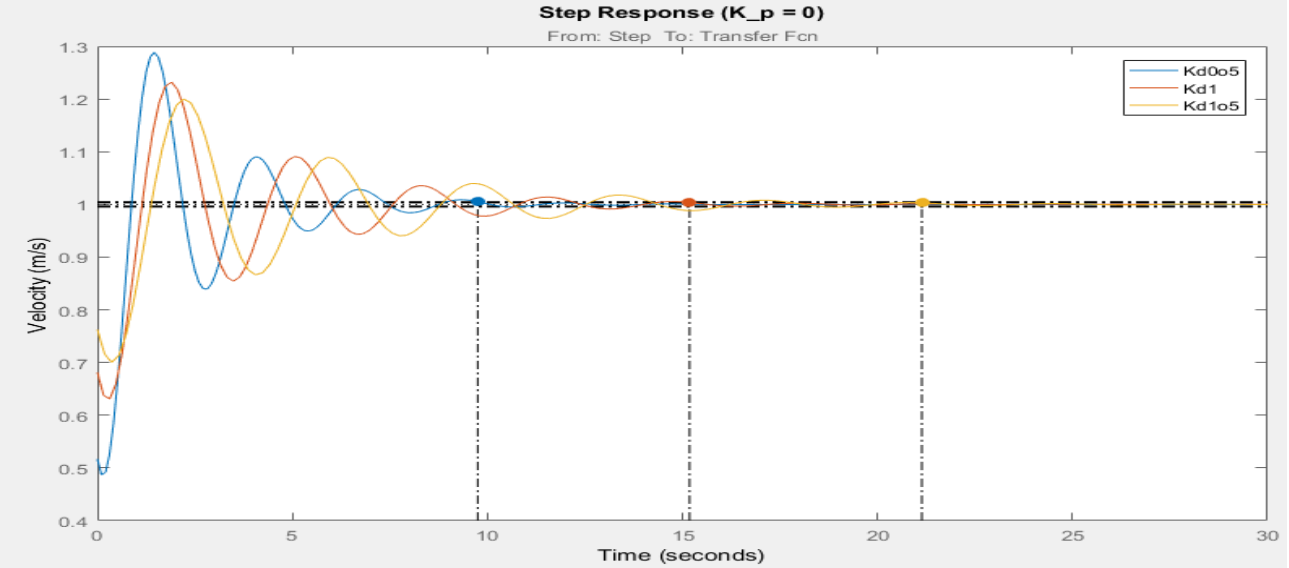

Figure 9: Step response with locked K_I at 5.72 and K_p set to zero.

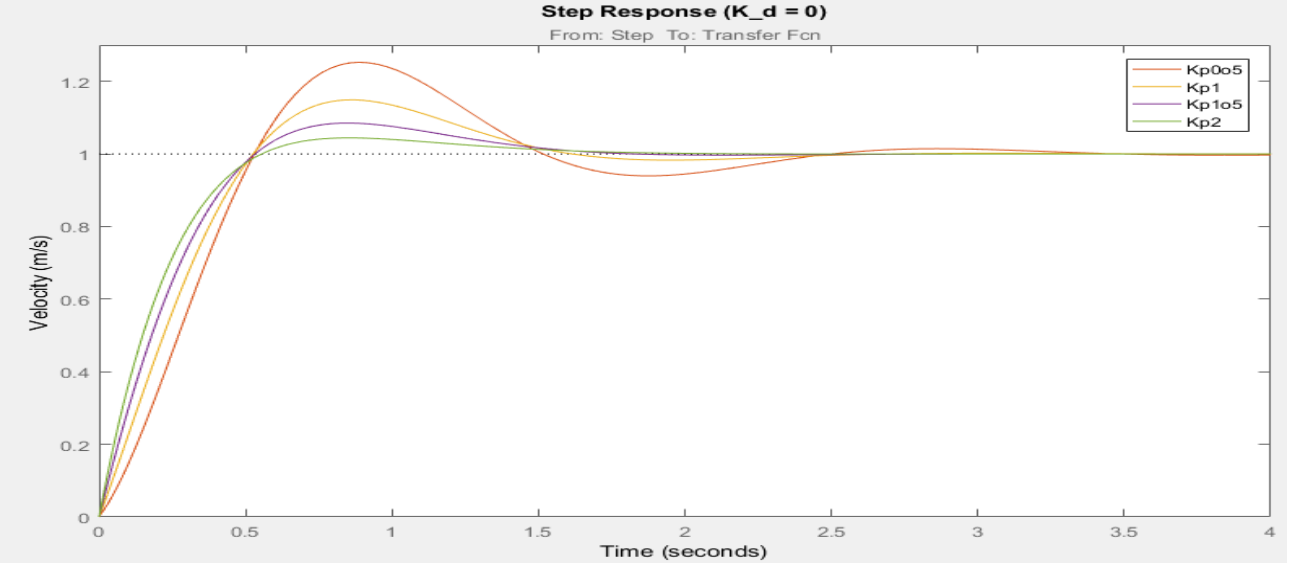

Figure 10: Step response with locked K_d at 5.72 and K_d set to zero.

APPENDIX E

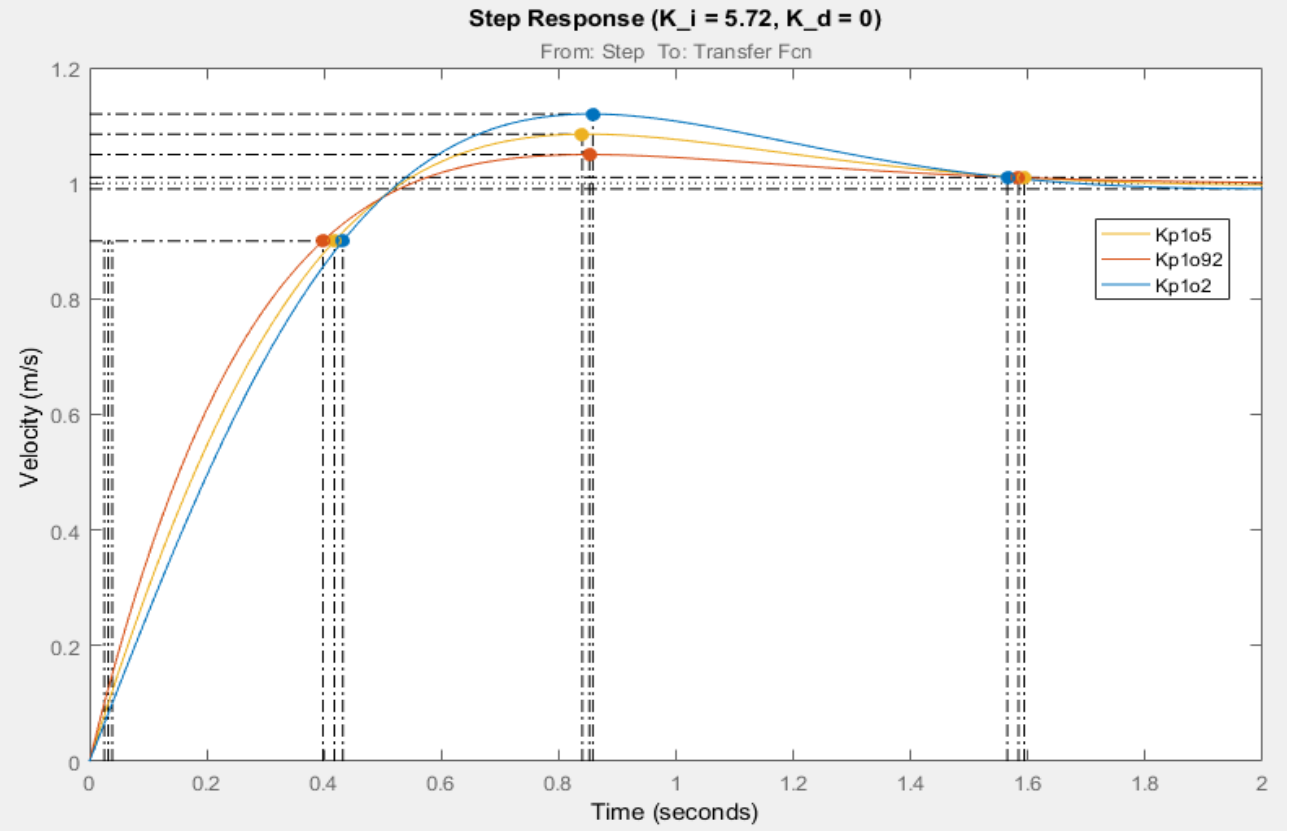

Figure 11: Selecting step response that meet the design requirement and to obtain the value of K_p.

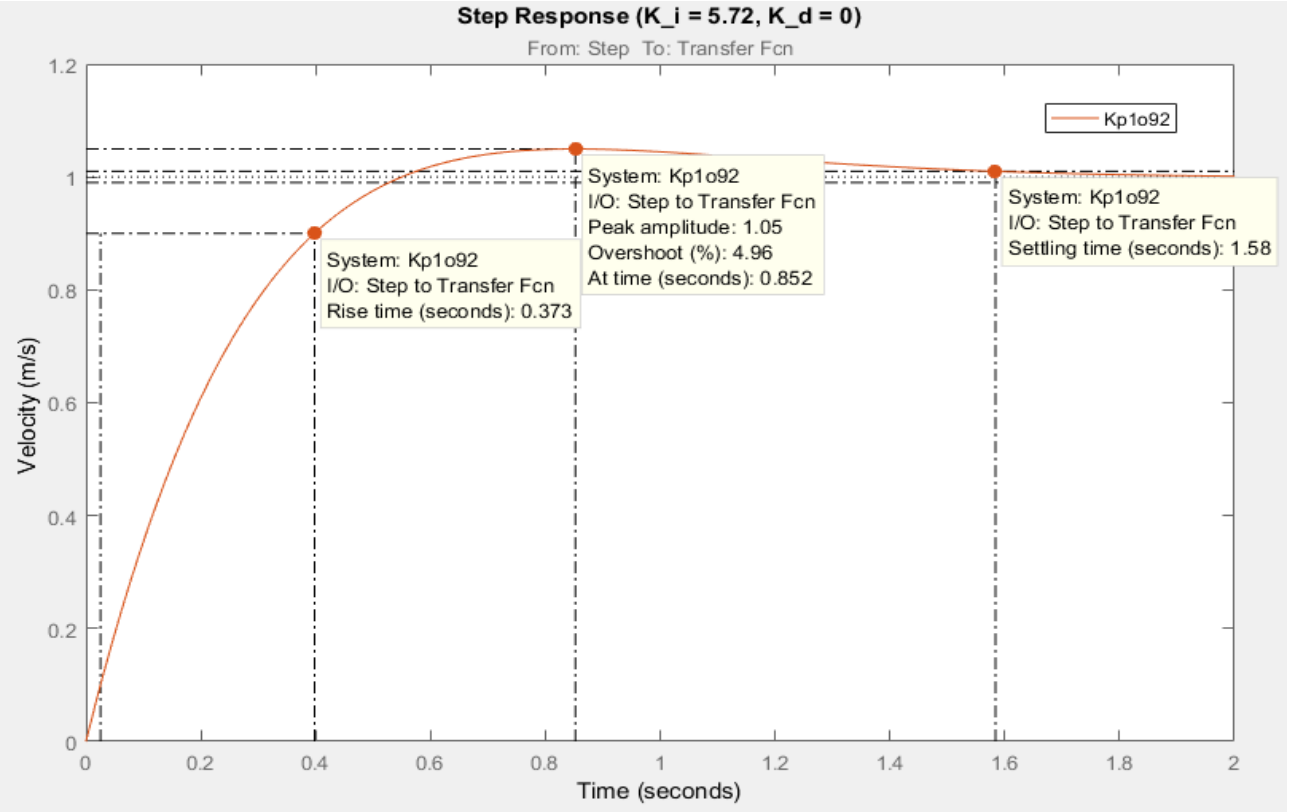

Figure 12: The final compensated system step response that satisfy the design requirements.

APPENDIX F

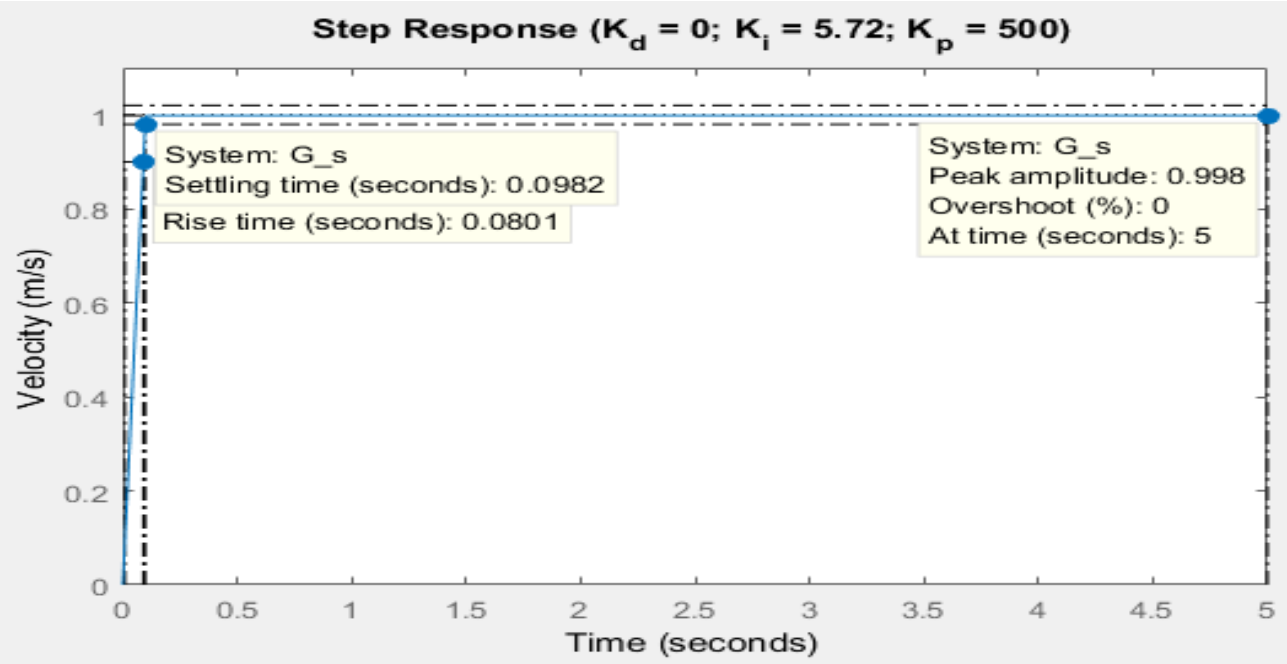

Figure 13: Step response for large value of K_p.

Mathematical proof that PI controller turn to P when K_p approaches infinity

Close loop transfer function of the first order plant compensated with PID controller is represented by equation 1 below.

$$G(s) = \frac{\frac{(K_p \cdot s + K_I + K_d s^2) \cdot K}{\tau + K_d \cdot K}}{s^2 + (\frac{1 + K_p \cdot K}{\tau + K_d \cdot K}) \cdot s + \frac{K_I \cdot K}{\tau + K_d \cdot K}} \tag{1}$$

Since the value of K_d is equal to zero the, system is now compensated by a PI controller instead PID which is shown by equation 2 below.

$$G(s) = \frac{\frac{(K_p \cdot s + K_I) \cdot K}{\tau}}{s^2 + (\frac{1 + K_p \cdot K}{\tau}) \cdot s + \frac{K_I \cdot K}{\tau}} \tag{2}$$

Dividing the numerator and denominator of (2) with K_p, and introducing the limit of K_p approaching infinity gives equation 3 below.

$$\lim_{K_p \to \infty} G(s) = \frac{\frac{K}{\tau} \cdot s + \frac{K_I K}{\tau K_p}}{\frac{1}{K_p} \cdot s^2 + \frac{1}{\tau K_p} \cdot s + \frac{K}{\tau} \cdot s + \frac{K_I K}{\tau K_p}} = \frac{\frac{K}{\tau} \cdot s}{\frac{K}{\tau} \cdot s} = 1 \tag{3}$$

With the results obtained in equation 3, it is clear that $K_p \gg K_I$ and therefore equation 3 under this conditions can be represented by equation 4 below.

$$G(s) = \frac{\frac{K_p K}{\tau} \cdot s}{s^2 + \frac{K_p K}{\tau} \cdot s} = \frac{K_p K}{\tau \cdot s + K_p K} \tag{4}$$

The results of equation 4 gives the close loop transfer function with P controller for a first order plant. The missing value of 1 in the denominator is due to fact that $K_p \gg 1$ and therefore that value add no significance.